Vol 11 No 6, June 2002
1009-1963/2002/11(06)/0583-04

Chinese Physics

© 2002 Chin. Phys. Soc.
and IOP Publishing Ltd

A new numerical method for the analysis of the permeability anisotropy ratio*

Xu You-Sheng(许友生)[a] and Xu Xian-Zhi(徐献芝)[b]

[a] *Department of Physics, College of Mathematics, Physics and Information Science, Zhejiang Normal University, Jinhua 321004, China*

[b] *Department of Mechanics, University of Science and Technology of China, Hefei 230026, China*

(Received 27 September 2001; revised manuscript received 26 January 2002)

By combining the lattice Boltzmann method with the three-dimensional computer-simulated images of porous media, a new numerical experimental methodology is used to determine the permeability anisotropy ratio of porous media. The results compare well with the laboratory experimental data.

Keywords: permeability anisotropy ratio, numerical experimental, image
PACC: 4755M, 0340G

1. Introduction

The delineation of the permeability anisotropy ratio plays an important role in studying the transport of fluids through porous media. Specifically, the physical characterization of the permeability in a porous medium is complex and remains formidable for a comprehensive solution. Attempts in the past have attacked it using various types of method, such as the mathematical methodology[1−4] and the permeameter measurements.[5−7] Recent advances in digital image processing have opened up new avenues to quantify and simulate the permeability anisotropy ratio of porous media.[8] The main focus of our paper is to present a full description of the permeability anisotropy ratio in a three-dimensional porous microstructure captured in a computer by using image-processing techniques and the lattice Boltzmann method. We also present a procedure for the simulation of the permeability anisotropy ratio based on permeameter measurements of the statistics of the anisotropic pore space distribution by making use of the full information obtained in our previous studies.

2.General method

The computer-simulated images of porous media were captured from resin-impregnated specimens with the aid of an optical microscope and an image analysis system. The flow model in a three-dimensional image of porous medium is shown in Fig.1. The fluid permeability is defined via Darcy's law[9]

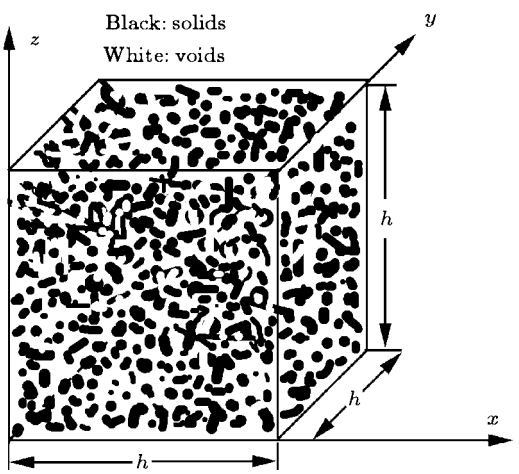


Fig.1. Three-dimensional section of the computer-simulated image of a porous medium, h=3mm.

$$\boldsymbol{V} = -\frac{1}{\mu}\boldsymbol{K}\cdot\nabla P, \tag{1}$$

where $\boldsymbol{V}$ is the average velocity vector within a sample, μ is the viscosity coefficient, $\nabla\boldsymbol{P}$ is the pressure gradient, and $\boldsymbol{K}$ is the symmetric positive definite permeability coefficient tensor. For a three-dimensional analysis of the images, Eq.(1) can be written as

$$\begin{bmatrix} u \\ v \\ w \end{bmatrix} = -\frac{1}{\mu h}\begin{bmatrix} K_{xx} & K_{xy} & K_{xz} \\ K_{yx} & K_{yy} & K_{yz} \\ K_{zx} & K_{zy} & K_{zz} \end{bmatrix}\begin{bmatrix} \Delta P_x \\ \Delta P_y \\ \Delta P_z \end{bmatrix}, \tag{2}$$

*Project supported by the National High Performance Computing Foundation of China (Grant No 970013), and by the Science Foundation of Jinhua, Zhejiang Province, China (Grant No 2001-1-157).

where u, v and w are the average velocities in an image in the x-, y- and z-directions, respectively, and h is the dimension of an image in pixels. The components of the permeability tensor are calculated in three steps. In the first step a pressure difference is applied in the x-direction ΔP_x, while ΔP_y=0 and ΔP_z=0, and K_{xx}, K_{xy} and K_{xz} are calculated as follows

$$K_{xx} = -\frac{(uh) \times u}{\Delta P_x}, \tag{3}$$

$$K_{yx} = -\frac{(uh) \times v}{\Delta P_x}, \tag{4}$$

$$K_{zx} = -\frac{(uh) \times w}{\Delta P_x}. \tag{5}$$

With the aid of the similarity of the second and third steps to the first step, the remaining coefficients of the tensor may be calculated as follows

$$K_{xy} = -\frac{(\mu h) \times u}{\Delta P_y}, \tag{6}$$

$$K_{yy} = -\frac{(\mu h) \times v}{\Delta P_y}, \tag{7}$$

$$K_{zy} = -\frac{(\mu h) \times w}{\Delta P_y}, \tag{8}$$

$$K_{xz} = -\frac{(\mu h) \times u}{\Delta P_z + \rho g}, \tag{9}$$

$$K_{yz} = -\frac{(\mu h) \times v}{\Delta P_z + \rho g}, \tag{10}$$

$$K_{zz} = -\frac{(\mu h) \times w}{\Delta P_z + \rho g}. \tag{11}$$

Here ρ is the fluid density and g is the gravitational acceleration. The average permeability $K_{\rm avg}$ is the first invariant of the permeability tensor

$$K_{\rm avg} = \frac{K_{xx} + K_{yy} + K_{zz}}{3}. \tag{12}$$

It should be noted that the absolute permeability K has units of (pixel)^2. It is multiplied by a pixel actual spatial volume ($\Delta x \Delta y \Delta z$) to convert it to the units of square meters. The absolute permeability tensor coefficients K are related to Darcy permeability tensor coefficients k with the units of m·s^{-1} by the following relationship

$$k = K\frac{r}{\mu}, \tag{13}$$

where r=9.81kN·m^{-3} is the unit weight of the fluid (water in our study) and μ is equal to 10^{-3}kg·ms^{-1} for water. The permeability coefficients are calculated in our study using the units of m·s^{-1}. The permeability anisotropy is measured by the ratio of the horizontal permeability coefficient $K_{\rm h}$ to the vertical permeability coefficient $K_{\rm v}$,

$$\gamma_K = \frac{K_{\rm h}}{K_{\rm v}}. \tag{14}$$

The anisotropy ratio γ_K is based on three-dimensional permeability calculations of 25 images captured on each test specimen. The ratio for the three-dimensional analysis was calculated by taking the average permeability in the two horizontal directions and dividing by the permeability in the vertical direction. From the knowledge of ΔP_x, ΔP_y, ΔP_z, μ, u, v and w, the permeability coefficients and permeability anisotropy ratio may then be solved from Eqs.(3)–(14).

We know that $\boldsymbol{\Delta P}$ and $\boldsymbol{V}$ may be determined from the continuity equation and the Navier–Stokes (momentum) equations. On the other hand, the lattice Boltzmann method (LBM) is a new numerical method for the solution of the Navier–Stokes equations.[10–13] It has been discussed so far only in two dimensions. The extension to three dimensions is straightforward. We just have to choose a three-dimensional lattice and calculate appropriate equilibrium distribution. In this paper, we introduce a model of the three-dimensional LBM with 15 velocities[14] for the simulation of three-dimensional fluid in a porous medium. The lattice velocities $\boldsymbol{c}_i$ are read as follows

$$-\text{rest particle} : \boldsymbol{c}_0 = (0,0,0), \tag{15}$$

$$-2-\text{particles} : \boldsymbol{c}_{1,2}, \boldsymbol{c}_{3,4}, \boldsymbol{c}_{5,6} = (\pm 2,0,0),(0,\pm 2,0),(0,0,\pm 2), \tag{16}$$

$$-\sqrt{3}-\text{particles} : \boldsymbol{c}_7, \cdots, \boldsymbol{c}_{14} = (\pm 1,\pm 1,\pm 1). \tag{17}$$

There are three different speeds: 1 time speed 0, 6 time speeds 2 and 8 time speeds $\sqrt{3}$. The even moments yield four independent equations for calculation of F_0, F_2, F_3 and $k_{\rm B}T$·m^{-1}.

$$-0.\ \text{moment} : \sum_i F_i = F_0 + 6F_2 + 8F_3 = \rho, \tag{18}$$

$$-2.\ \text{moment} : \sum_i \boldsymbol{c}_{ix}^2 F_i = 8F_2 + 8F_3 = \rho\frac{k_{\rm B}T}{m}, \tag{19}$$

$$-4.\ \text{moment} : \sum_i \boldsymbol{c}_{ix}^4 F_i = 32F_2 + 8F_3 = 3\rho\left(\frac{k_{\rm B}T}{m}\right)^2, \tag{20}$$

$$\sum_i \boldsymbol{c}_{ix}^2 \boldsymbol{c}_{iy}^2 F_i = 8F_3 = \rho_6\left(\frac{k_{\rm B}T}{m}\right)^2. \tag{21}$$

The solution may be read

$$F_0 = \frac{7}{18}\rho, \tag{22}$$

$$F_2 = \frac{\rho}{16}\left(\frac{k_{\rm B}T}{m}\right)^2 = \frac{\rho}{36}, \tag{23}$$

$$F_3 = \frac{\rho}{8}\left(\frac{k_{\rm B}T}{m}\right)^2 = \frac{\rho}{18}, \tag{24}$$

$$\frac{k_{\rm B}T}{m} = \frac{2}{3}, \tag{25}$$

where F_i are the global equilibrium distributions, m is particle mass, $k_{\rm B}$ is Boltzmann constant, and T is temperature. The odd velocity moments over F_i vanish. The equilibrium distributions are not unique and other choices are possible. We choose the equilibrium distribution proposed by Chen *et al*[14]

$$F_0^{\rm eq} = d^{(0)} + \delta^{(0)}\boldsymbol{V}^2, \tag{26}$$

$$\begin{aligned} F_i^{\rm eq} =& d^{(1)} + \beta^{(1)}\boldsymbol{c}_i\cdot\boldsymbol{V} + \gamma^{(1)}(\boldsymbol{c}_i\cdot\boldsymbol{V})^2 + \delta^{(1)}\boldsymbol{V}^2 \\ & i = 1,\cdots,6, \end{aligned} \tag{27}$$

$$\begin{aligned} F_i^{\rm eq} =& d^{(2)} + \beta^{(2)}\boldsymbol{c}_i\cdot\boldsymbol{V} + \gamma^{(2)}(\boldsymbol{c}_i\cdot\boldsymbol{V})^2 + \delta^{(2)}\boldsymbol{V}^2 \\ & i = 7,\cdots,14, \end{aligned} \tag{28}$$

where

$$d^{(0)} = d^{(1)} = \frac{\rho}{11}, \quad d^{(2)} = \frac{\rho}{22}, \tag{29}$$

$$\alpha^{(1)} = \frac{\rho}{24}, \quad \alpha^{(2)} = \frac{\rho}{12}, \tag{30}$$

$$r^{(1)} = \frac{\rho}{32}, \quad r^{(2)} = \frac{\rho}{16}, \tag{31}$$

$$\delta^{(0)} = -\frac{7}{24}\rho, \quad \delta^{(1)} = -\frac{\rho}{48}, \quad \delta^{(2)} = -\frac{\rho}{24}. \tag{32}$$

Combining the principle of Bhatnagar, Gross and Krook (BGK) approximation, we can write the time evaluation of our lattice Boltzmann equations as

$$F_i(t+\Delta t) - F_i(t) = -\frac{1}{\tau}(F_i - F_i^{\rm eq}), \tag{33}$$

$$\rho = \sum_{i=1}^{14} F_i = \sum_{i=1}^{14} F_i^{\rm eq}, \tag{34}$$

$$\rho\boldsymbol{V} = \sum_{i=1}^{14}\boldsymbol{c}_i F_i = \sum_{i=1}^{14}\boldsymbol{c}_i F_i^{\rm eq}, \tag{35}$$

$$\begin{aligned} \rho\varepsilon =& \frac{1}{2}\sum_{i=0}^{14}(\boldsymbol{c}_i - \boldsymbol{V})^2 F_i \\ =& \frac{1}{2}\sum_{i=0}^{14}(\boldsymbol{c}_i - \boldsymbol{V})^2 F_i^{\rm eq}. \end{aligned} \tag{36}$$

Here $i = 1,\cdots,14$, τ is relaxation time, and ε is internal energy.

By taking large scale averages from the lattice, the full Navier–Stokes equations may be approximated by a Chapman–Enskog series expansion[15]

$$\begin{aligned} & \partial t\boldsymbol{V} + (\boldsymbol{V}\cdot\nabla)\boldsymbol{V} \\ =& -\frac{1}{\rho}\nabla P + \frac{\eta}{\rho}\nabla^2\boldsymbol{V} \\ & + \frac{1}{\rho}\left(\varepsilon + \frac{D-2}{D}\eta\right)\nabla(\nabla\cdot\boldsymbol{V}). \end{aligned} \tag{37}$$

Here D is dimensionality (in our study D=3),

$$\eta = \frac{2\tau - 1}{8}\rho, \tag{38}$$

$$\zeta = \frac{4\tau - 1}{8}(1 - 2C_{\rm s}^2)\rho, \tag{39}$$

where $C_{\rm s}$ is sonic velocity.

We know that, to a certain degree, achieving self-consistent boundary conditions with a given accuracy is as important as developing numerical schemes themselves. The implementation of boundary conditions for this paper is discussed in the following.

In general, there are two ways to define a boundary: the boundary curve may include grid nodes (node boundary[16]) or passes through the midpoint of links between nodes (link boundary[17]). Node boundaries are appropriate for periodic and inflow boundary conditions even in complicated geometry such as porous media. For our image (Fig.1), the boundary conditions are

$$F_i(x=0) = F_i(x=h), \tag{40}$$

$$F_i(y=0) = F_i(y=h), \tag{41}$$

$$F_i(z=0) = F_i(z=h). \tag{42}$$

Also, "no-slip" boundary conditions are applied by using the "bounce-back" boundary conditions.[18] A pressure difference is applied across the lattice by adding a fixed amount of momentum to the sites at one side of the lattice.

3. Conclusions and discussion

The permeability tensor coefficients, average permeability and permeability anisotropy ratio were calculated for images captured on the computer-modelled specimens. A total of 25 images were analysed for each

of the three specimens of sand, silica soil and glass beads. The average permeability coefficient k_{av} and permeability anisotropy ratio are reported in Table 1. It shows that the anisotropy ratio is the highest for silica soil. This is expected since silica soil is composed of elongated particles, while sand is composed of subrounded particles, and glass beads are completely spherical.

Table 1. Values of permeability and permeability anisotropy ratio from numerical analysis and laboratory data.

Source	Specimens	Permeability $k_{av}/10^{-5}cm^2$	Permeability anisotropy ratio	Comments
Laboratory	Sand	0.101	1.17∼1.26	Based on
(each specimen	glass beads	0.224	1.23∼1.29	permeameter
tested 20 times)	silica soil	0.122	1.60∼1.71	testing
	Sand	0.112	1.21	Using three-
Numerical	glass beads	0.228	1.27	dimensional
	silica soil	0.124	1.67	images

The permeability anisotropy was found to be correlated with particle elongation. In addition, the permeability anisotropy ratio is in the same range as the results of laboratory measurements. These improvements in permeability prediction in comparison with other analytical models are attributed to incorporating the effects of porous media microstructure on water flow directly into the solution through boundary conditions. There were no assumptions imposed on the shape of the pore structure.

References

[1] Rothman D H 1988 *Geophys.* **53** 509
[2] Chen S *et al* 1991 *Phys.* D **47** 72
[3] Shan X W and Chen H 1993 *Phys. Rev.* E **47** 1815
[4] Yan G W *et al* 1997 *Chin. J. Comput. Phys.* **14** 65 (in Chinese)
[5] Chapuis *et al* 1989 *J. Geotech.* **26** 614
[6] Martys N S *et al* 1994 *Phys. Rev.* E **50** 403
[7] Tian J P and Yao K L 2001 *Chin. Phys.* **10** 128
[8] Masad E and Muhunthan B 2000 *J. Geotech. Geoenviron. Eng.* **3** 126
[9] Kong X Y 1999 *Advanced Mechanics of Fluids in Porous Media* (Hefei: University of Science and Technology of China) p 37 (in Chinese)
[10] Namara G M and Zanetti G 1988 *Phys. Rev. Lett.* **61** 233 2
[11] Yu H D and Zhao K H 1999 *Acta Phys. Sin.* **48** 1470 (in Chinese)
[12] Li H B *et al* 2000 *Acta Phys. Sin.* **49** 392 (in Chinese)
[13] Yu H D and Zhao K H 2000 *Acta Phys. Sin.* **49** R818 (in Chinese)
[14] Chen S Z *et al* 1992 *J. Stat. Phys.* **68** 379
[15] Wolfram S 1986 *J. Stat. Phys.* **45** 471
[16] Inamuro T *et al* 1995 *Phys. Fluids* **72** 928
[17] Ladd A J C 1994 *J. Fluid Mech.* **271** 285
[18] Cournubert R *et al* 1991 *Phys.* D **47** 241